Journal of Solid State Chemistry **158,** 25–33 (2001)
doi:10.1006/jssc.2000.9052, available online at http://www.idealibrary.com on IDEAL®

Crystal Growth and Intergrowth Structure of the New Heavy Fermion Materials $CeIrIn_5$ and $CeRhIn_5$

E. G. Moshopoulou,*,†,[1] Z. Fisk, *,‡ J. L. Sarrao,* and J. D. Thompson*

*Los Alamos National Laboratory, Los Alamos, New Mexico 87545; †Brookhaven National Laboratory, Upton, New York 11973; and ‡National High Magnetic Field Laboratory, Florida State University, Tallahassee, Florida 32306

Received July 24, 2000; in revised form November 14, 2000; accepted December 8, 2000

The structures of the new heavy fermion materials $CeIrIn_5$ and $CeRhIn_5$ have been determined by single-crystal neutron ($R(F) = 0.051$) and X-ray ($R(F) = 0.056$) diffraction, respectively. Both compounds adopt tetragonal structure, space group *P4/mmm* (No. 123), $Z = 1$, $a = b = 4.674(1)$ Å, and $c = 7.501(5)$ Å for $CeIrIn_5$, and $a = b = 4.656(2)$ Å, and $c = 7.542(1)$ Å for $CeRhIn_5$. The possible presence of antisite disorder, a long-standing question on this type of structure, was excluded by both electron and neutron or X-ray diffraction. The compounds are built by monolayers of face-sharing distorted cuboctahedra [$CeIn_3$] and monolayers of edge-sharing rectangular parallelepipeds [$RhIn_2$] or [$IrIn_2$], stacked alternatively in the [001] direction. Therefore, they are new members of the inhomogeneous linear homologous series $M_mT_nT'_{3m+2n}$. Because of their ordered intergrowth structure, the physical properties of the quasi-two-dimensional heavy electron systems $CeIrIn_5$ and $CeRhIn_5$ can be directly compared with the corresponding ones of their parent compound, the three-dimensional heavy fermion material $CeIn_3$. © 2001 Academic Press

Key Words: **heavy fermion; lattice dimensionality; diffraction; intergrowth structure; homologous series.**

I. INTRODUCTION

The discovery of new heavy fermion materials, with novel physical behavior and unusual crystal structures, is a key to unlocking the solution to fundamental problems in the physics of highly correlated electron states of condensed matter. Such problems include superconductivity, magnetism, the relationship between these two phenomena, and heavy fermion behavior. Over the past 20 years, the search for new heavy electron materials was only partially guided by knowledge of the structure–property relationship, i.e., what structures are better suited to the formation of a heavy electron ground state and what chemical and structural features favor heavy fermion behavior. References (1–4) discuss chemical and structural regularities in the class of heavy fermion materials. Besides this rational approach, exploratory synthesis yielded exciting new materials with unexpected structures and properties. The myriad of experiments devoted to explore all compounds, obtained by either rational or exploratory synthesis, revealed that heavy fermion materials are very complex and rich in both their physics and crystal chemistry: they not only adopt an extreme diversity of crystal structures but also exhibit a wide variety of ground states ranging from exotic superconductors to magnets as well as to unusual semiconductors. All these systems provide an appropriate experimental environment to study the basic and broad problems of superconductivity, magnetism, and heavy fermion behavior. However, more specific questions could not yet be addressed through the known heavy fermion materials. One such question is what structural features, for example, lattice dimensionality, various types of structural disorder, etc. are relevant to the heavy fermion behavior and in what way do they influence cooperative phenomena. Recently, we discovered two new heavy fermion materials, $CeIrIn_5$ and $CeRhIn_5$, which open new possibilities to address the long-standing question of the role of spatial dimensionality on the low-temperature behavior of heavy electron systems. Both materials exhibit unusual behavior and adopt a novel (for a heavy fermion) crystal structure governed though by the same structural principles as those of the known heavy fermion materials, $CeIn_3$.

$CeIrIn_5$ and $CeRhIn_5$ have been investigated by magnetic susceptibility, electrical resistivity, and specific heat, down to very low temperatures (≈ 50 mK) and/or up to relatively high pressures (≈ 22 kbar). The detailed results of these experiments were reported elsewhere (5, 6). $CeIrIn_5$ is a heavy fermion superconductor at ambient pressure with a bulk superconducting transition temperature, $T_c = 0.4$ K, and electronic coefficient of specific heat $\gamma \equiv C/T \approx 750$ mJ/(mol K^2) above T_c. It is the first ambient pressure heavy fermion superconductor discovered since 1991 (when UPd_2Al_2 was discovered) and the second example of lanthanide-based, ambient pressure, heavy fermion

[1] To whom correspondence should be addressed. E-mail: evagelia@ims.demokritos.gr. Fax: +30-1-6519430.

0022-4596/01 $35.00

superconductor discovered 20 years after the first one, $CeCu_2Si_2$, opened the field of heavy fermion physics and particularly the area of heavy fermion superconductivity. The temperature dependencies of the specific heat and thermal conductivity of $CeIrIn_5$ below T_c are clearly not those expected of BCS superconductivity. $CeRhIn_5$ exhibits heavy electron behavior with $C/T \geq 420$ mJ/(mol K^2) and orders antiferromagnetically at $T_N = 3.8$ K. Application of hydrostatic pressure of about 16.3 kbar induces a first-order-like transition from an unconventional antiferromagnetic state to a superconducting state with $T_c = 2.1$ K (Ref. (6)). The evolution from antiferromagnetic to superconducting states is striking in that it does not follow widely accepted theoretical predictions (7) and is markedly different from any previously reported for a heavy fermion compound. Our first structural characterization of single crystals of $CeIrIn_5$ and $CeRhIn_5$ by conventional powder X-ray diffraction led to the significant observation that both compounds are new members of the inhomogeneous linear homologous series $M_mT_nT'_{3m+2n}$, an intergrowth structure series initially reported by Grin *et al.* (8).

This paper reports the crystal structure behind these unique materials, deduced from structural refinements based on single-crystal X-ray and neutron diffraction data. Besides establishing the crystal structure, a mandatory first step when a new material is discovered, an additional and perhaps more important aim of this study is to determine the relationship among crystallographic parameters of $CeIrIn_5$ and $CeRhIn_5$ and the corresponding ones of $CeIn_3$, the parent compound of their homologous series $Ce_m(Rh,Ir)_nIn_{3m+2n}$. In this way, this structural study can provide critical information for testing theories that explain the behavior of the various members of the series and eventually for guiding the discovery of new materials $M_mT_nT'_{3m+2n}$ with novel or enhanced properties.

Despite their relatively simple chemical formula, the determination of the accurate crystal structure of $CeIrIn_5$ and $CeRhIn_5$ presents two principal difficulties: first, both materials have very high absorption coefficients for either X-ray or neutron radiation, and second, some of their atoms do not have sufficient differences in either their neutron or X-ray scattering factors. Our approach to overcome these difficulties was to combine electron, neutron, and X-ray diffraction. Electron diffraction has been used to check for weak effects like diffuse scattering or superstructure, which due to the problems just mentioned, would be hardly observed by X-rays or neutrons.

II. EXPERIMENTAL

II.1. Crystal Growth and Characterization by Conventional Powder X-ray Diffraction

Single crystals of the title compounds were grown by combining high-purity Ce, Ir or Rh, and In (all constituents had purities of 99.95% or better) in the ratio 1:1:20, placing these materials in an alumina crucible and encapsulating the crucible in an evacuated quartz tube. The resulting ampoule was heated over several hours to 1100°C, allowed to equilibrate for 2 h, and then slow-cooled (10°C/h) to 700°C. At this point the excess In flux was decanted in a centrifuge, leaving well-separated single crystals (9). Most of the crystals show columnar habit, with their long axis along the tetragonal c axis.

The powder X-ray diffraction spectrum of ground crystals of each compound was obtained with a Scintag diffractometer using monochromatic Cu$K\alpha$ radiation. Silicon powder was used as an internal standard. The powder patterns could be indexed unambiguously, assuming the compounds to be of the $HoCoGa_5$-type structure (8), space group $P4/mmm$ (D^1_{4h}, No. 123), and $Z = 1$. Comparison of the observed spectra with the theoretical ones (calculated with the LAZY PULVERIX program (10)) did not reveal significant discrepancies in the relative intensities.

The positions, FWHM's and intensities of several peaks were obtained from fits to a Pearson VII peak shape function (11). By expressing the evolution of the FWHM of the peaks as a function of 2θ, the Williamson–Hall function (12), i.e. (sin θ) versus ($\mathrm{Fwhm_{intr}} \times \cos\theta$), was estimated; here, $\mathrm{Fwhm_{intr}}$ is the "intrinsic" Fwhm of the peaks of the sample (i.e., obtained after subtracting the instrumental function). From the Williamson–Hall plot (12), it is deduced that the crystalline strain is $\varepsilon \approx 0.7 \times 10^{-3}$ for $CeIrIn_5$ and $\varepsilon \approx 0.9 \times 10^{-3}$ for $CeRhIn_5$; i.e., the strain is very low in both these materials. This result is also consistent with the sharpness of the X-ray diffraction peaks (the Fwhm of almost all the peaks is no more than twice that of Si), an observation that also demonstrates the very good quality of the materials. The cell parameters were obtained by least-squares refinement of the reciprocal space positions of ten well-separated reflections in the range $2\theta = 34°$ to 74°. The resulting lattice constants are $a = b = 4.674(1)$ Å and $c = 7.501(5)$ Å for $CeIrIn_5$ and $a = b = 4.656(2)$ Å and $c = 7.542(1)$ Å for $CeRhIn_5$.

II.2. Electron Diffraction Study of $CeIrIn_5$ and $CeRhIn_5$

The aim of the electron diffraction experiments was to check for possible static order/disorder and/or superstructure effects in these compounds. Such effects might occur in our samples for the following reason: $CeRhIn_5$ and $CeIrIn_5$ contain $PtHg_2$-type "cubes", "$RhIn_2$" and "$IrIn_2$", respectively. In this type of structural unit (and consequently in the structural series containing it) there is some doubt about the extent of ordering of the constituent atoms (13–15).

Because of the similarity in X-ray scattering factors of Rh and In, any site disorder between Rh and In in $CeRhIn_5$ would be hardly observable by single-crystal X-ray diffraction. On the other hand, since the neutron scattering lengths

of In and Ir are sufficiently different, an eventual site disorder between In and Ir in $CeIrIn_5$ should be deduced from the refinement of the neutron diffraction data. However, both compounds present high absorption coefficients for neutron and X-ray radiation, which could hinder detection of weak superstructure reflections and diffuse intensity. Therefore, electron diffraction experiments are useful for both materials. Clarification of the issue of site disorder in a heavy fermion material is very important because it is known (2, 16) that the *f* element's local chemical environment has strong influence on the behavior of a heavy electron system. Even more significantly, the possible presence of site disorder in $CeIrIn_5$ and $CeRhIn_5$ would prohibit their comparison with their parent compound $CeIn_3$.

Before turning to the details of the electron diffraction experiments, it is worth noting here that these experiments aim to search for rather periodic effects like superstructure reflections and almost periodically modulated diffuse intensity between the Bragg spots. If such effects indeed exist, then, through reconstruction of the reciprocal space, the type of the anti-site-disorder can be deduced. Hence, the electron diffraction study is to a large extent complementary to the residual resistivity measurements (17), which reflect scattering from random defects (like dislocations, impurities, grain boundaries, random anti-site-disorder, etc.) that might exist in the materials. Nearly periodic "disorder" might have no or very little effect on the residual resistivity. For example, in the heavy fermion compound $CeInCu_2$, nearly periodic "disorder" (observed as almost periodically modulated diffuse intensity in the reciprocal space) does not influence the residual resistivity, even if it remains at low temperature (18). The residual resistivity of $CeRhIn_5$ and $CeIrIn_5$ is low, of the order 1 $\mu\Omega$-cm, suggesting that they are nearly defect-free materials (17).

Specimens of $CeIrIn_5$ and $CeRhIn_5$ were prepared for electron diffraction by grinding the crystals in an agate mortar under methanol. A drop of the resulting suspension was placed on a copper grid coated with holey-carbon film. Electron diffraction studies were performed on a Philips CM30 transmission electron microscope operated at 300 kV and equipped with a KEVEX X-ray energy-dispersive spectrometer (XEDS).

Several "beam-transparent" areas along the edges of many crystallites of each compound were initially examined by XEDS to check both the homogeneity and the stability under the e-beam of the specimens. All the crystallites were studied under kinematical diffraction condition. The XEDS spectra were acquired, for all the crystallites, under the same conditions of electron beam energy, detector efficiency, collecting time (1000 s for each spectrum), position, and orientation of the specimen relative to the detector. Comparison of the obtained spectra of each compound did not reveal any significant difference in the relative intensities of the elements, suggesting therefore absence of any composition gradients (within experimental accuracy of $\approx 5\%$) in the crystals.

Selected area diffraction (SAD) patterns were taken along several zone axes for many very thin crystallites of both samples. As an example, the pattern of $CeIrIn_5$ in the $[\bar{1}12]$ beam direction and the pattern of $CeRhIn_5$ in the $[\bar{2}01]$ beam direction are given in Fig. 1. All diffraction spots could be indexed by using the cell parameter: $a = b = 4.674(1)$ Å and $c = 7.501(5)$ Å for $CeIrIn_5$, and $a = b = 4.656(2)$ Å and $c = 7.542(1)$ Å for $CeRhIn_5$, obtained from the refinement of the powder X-ray diffraction data. No diffuse streaks between the Bragg spots or extra reflections violating the space group $P4/mmm$ have been observed. The diffraction spots do not appear elongated or split, indicating absence of any disoriented adjacent

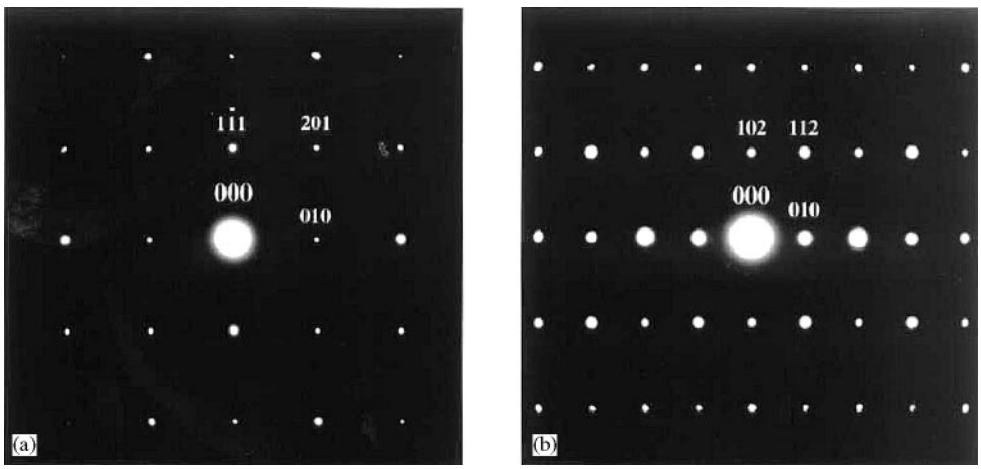

FIG. 1. Electron diffraction pattern of (a) a $CeIrIn_5$ crystallite in the $[\bar{1}12]$ electron beam direction and (b) a $CeRhIn_5$ crystallite in the $[\bar{2}01]$ electron beam direction.

domains in the crystallites. Consequently, the strain in the materials is very low, consistent with results of the powder X-ray diffraction experiments.

The absence of diffuse intensity between the Bragg reflections on the electron diffraction patterns demonstrates that no anti-site-disorder exists in $CeRhIn_5$ and $CeIrIn_5$ and therefore classic single-crystal X-ray or neutron diffraction can be employed to determine accurately the crystallographic parameters of these materials. This study is presented in the next section, which is devoted to the determination of the crystal structure of $CeIrIn_5$ and $CeRhIn_5$.

II.3. Determination of the Crystallographic Parameters of $CeIrIn_5$ and $CeRhIn_5$

II.3.1. Neutron Diffraction Study of $CeIrIn_5$

Data acquisition. Time-of-flight neutron diffraction data were collected at the Intense Pulsed Neutron Source (IPNS) at Argonne National Laboratory using the single-crystal diffractometer equipped with a position-sensitive ^{6}Li-glass scintillation area (30×30 cm) detector. Details of the technique and the data collection and analysis procedures are given in Refs. (19–22). The crystal selected for the neutron diffraction experiment was an almost right parallelepiped with its faces (100) and (-100) at 0.094 cm, (010) and $(0-10)$ at 0.088 cm, and (001) and $(00-1)$ at 0.05 cm from the center of the crystal. It was mounted at the end of an aluminum pin and centered in the beam. Local Argonne programs were used for the data acquisition. Initially, three histograms were collected at different χ and ϕ setting angles to examine the crystal quality and to obtain an orientation matrix. The orientation matrix was obtained by an auto-indexing procedure using data obtained by searching the histogram for peaks. The instrument uses ω fixed at 45° and different volumes of reciprocal space are recorded by setting ϕ and χ at a number of values. Thirteen diffractometer settings were used to obtain at least one unique quadrant of reciprocal space. For each setting of the diffractometer angles, data were stored in a three-dimensional histogram form with coordinates x, y, and t corresponding to horizontal detector position, vertical detector position, and the time of flight, respectively. The 120 time-of-flight histogram channels were constructed with constant $\Delta t/t = 0.015$ and correspond to wavelengths of 0.7–4.2 Å.

Data reduction. The IPNS-SCD single-crystal analysis package (22) was used in all steps of the data reduction. The positions and indices of reflections in each histogram were predicted from the orientation matrix. All peaks could be successfully indexed and no splitting was observed at the high q reflections, indicating that the crystal was single. Then, the regions around the predicted positions were integrated in three dimensions. For the integration we used a modified version of the program "Integrate" (23), which checks for overlaps, deconvolutes, subtracts the intensities due to individuals other than the crystal, and then performs the integration of the intensities diffracted only by the crystal. Unit cell parameters of $a = 4.673(1)$ Å, $c = 7.505(3)$ Å, and $\alpha = \beta = \gamma = 90.002(1)^\circ$ were obtained from a least-squares fit of the observed centroid positions of all reflections of all histograms, i.e., total of 802 Bragg peaks. The cell parameters obtained from the X-ray study are $a = b = 4.674(1)$ Å, $c = 7.501(5)$ Å, and $\alpha = \beta = \gamma = 90^\circ$.

Then, the net integrated intensities were corrected for Lorentz factor and normalized by taking into account the known measured spectral distribution of the incident beam, the detector efficiency, and dead-time losses. The wavelength-dependent numerical absorption $A(\lambda)$ correction was calculated using the precise size of the crystal and the Miller indices of its faces and considering the neutron absorption cross sections of the elements from Sears (24). $A(\lambda)$ was then applied to each reflection. Symmetry-related reflections were not averaged since different extinction factors were applicable to reflections measured at different wavelengths.

Refinement of the structure. The initial structural model was the structure of $UCoGa_5$ obtained from (25), i.e., Ce at 1*a* (000), Ir at 1*b* (00$\frac{1}{2}$), In1 at 1*c* ($\frac{1}{2}\frac{1}{2}$0) and In2 at 4*i* (0$\frac{1}{2}$0.31). Refinements, based on the structure factor amplitude F, were performed using the least-squares refinement program GSAS (26). All reflections of $I > 3\sigma(I)$, i.e., total of 540 observations, were included in the refinement. Initially, only the 13 scale factors (1 for each histogram of data) were refined, resulting in residual $R_w(F) = 32.1\%$, but subsequent refinements of the positional parameter of z of In2 and then also of isotropic thermal factors of all atoms led to $R_w = 7.4\%$. In the next few refinement cycles, a secondary extinction correction (Becker and Coppens formalism (27) type I, Lorentzian distribution) was included and refined together with the scale factors, the z of In2, and anisotropic thermal factors of all atoms (28). The occupancy factors of all atoms were also varied but as their final values were equal to 1 (within the experimental precision), they were subsequently fixed to 1. The obtained R_w and goodness-of-fit GOF $= \chi^2$ were 6.2% and 2.811, respectively. Site disorder between Ir and In2 was introduced into the model but the residuals were significantly larger. Also, possible substitution of the empty 1*d* ($\frac{1}{2}\frac{1}{2}\frac{1}{2}$) site by Ir and/or In2 was checked but the obtained residuals were very high. Therefore, Ir and In2 were placed again in their previous sites 2*b* and 4*i* of the ordered structure. In the final cycles a robustness criterion was used; i.e., all weights were scaled by $\min(F_{obs}/F_{calc}, F_{calc}/F_{obs})^4$; in this way the very few "outlier" reflections are down-weighted in the refinement. This modification on the weighting of the reflections did not alter the structural parameters, although it improved the residuals, i.e., $R_w = 0.050$ and $\chi^2 = 1.551$. The least-square refinement

TABLE 1
Parameters of the Least-Squares Refinement of the Single Crystal Neutron Diffraction Data

Number of reflections (all data)	802
Number of reflections with $I > 3\sigma(I)$	540
Number of parameters varied for data $I > 3\sigma(I)$	24
Range of scale factors	14.3(2)–16.34(1)
Extinction parameter g (rad^{-1})	$2.4(1) \times 10^{-5}$
Linear absorption coefficient (cm^{-1})	$\mu = 0.183 + 4.714\lambda$
$R(F)$	0.051
$R_w(F)$	0.082
GOF $\equiv \chi^2$ (based on F)	1.552

Note. The single crystal function minimized was $\sum w_i(|F_{obs}| - S|F_{calc}|)^2$, where $w_i = (2F_{obs}/\sigma(F_{obs}^2))^2 \times \min(F_{obs}/F_{calc}, F_{calc}/F_{obs})^4$ is the individual weight and S is the scale factor. $R(F) = \sum||F_{obs}| - S|F_{calc}||/\sum|F_{obs}|$, $R_w(F) = [\sum w_i(|F_{obs}| - S|F_{calc}|)^2/\sum w_i|F_{obs}|]^{1/2}$, and GOF $\equiv \chi^2 = \sum w_i(|F_{obs}| - S|F_{calc}|)^2/(N_{obs} - N_{var})$, where N_{obs} = number of observations and N_{var} equals number of variables.

parameters are listed in Table 1. The final positional parameters, thermal factors, and occupancy factors are given in Table 2. Selected interatomic distances and important angles are given in Table 3. The lists of observed and calculated structure factors are omitted, but they are available upon request.

II.3.2. Single-Crystal X-ray Diffraction Study of $CeRhIn_5$

Data acquisition. The crystal selected for the X-ray diffraction experiment was an almost right parallelepiped with dimensions 0.58, 0.21, and 0.08 mm. This thickness is very close to the optimum one estimated from the absorption coefficient ($\mu = 26.455\ mm^{-1}$) of $CeRhIn_5$ for $\lambda_{MoK\alpha}$ radiation. The crystalline quality of this sample was first checked at a precession camera and then placed on an automatic, computer-controlled, four-circle Bruker P4/CCD/PC diffractometer using Mo$K\alpha$ radiation and a graphite monochromator. The cell parameters were refined by the least-squares method using the absolute θ angle of 18 high-angle reflections. The resulting values are $a =$ 4.6551(5) Å, $c = 7.5426(11)$ Å, and $\alpha = \beta = \gamma = 90.001(2)^\circ$. A hemisphere of data was collected ($\theta = 2.7^\circ$ to 26.31°) using a combination of ϕ and ω scans, with 30-s frame exposures and 0.3° frame widths. Data collection was handled using SMART software (29). Frame integration and final cell parameter calculation were carried out using SAINT software (30). The final cell parameters were determined by the least-squares method using the absolute θ angle of 853 reflections. The stability of the beam, of the equipment, and of the crystal was monitored by measuring two standard reflections at intervals of 40 reflections.

TABLE 2
Atomic Coordinates and Thermal Factors for $CeIrIn_5$

Atom	x	y	z	U_{11} (Å^2)	U_{22} (Å^2)	U_{33} (Å^2)
Ce	0	0	0	0.00452(63)	0.00452(63)	0.00622(82)
Ir	0	0	0.5	0.00315(36)	0.00315(36)	0.00539(46)
In1	0.5	0.5	0	0.00748(80)	0.00748(80)	0.0159(12)
In2	0	0.5	0.30524(18)	0.01606(75)	0.00478(62)	0.00755(59)

Note. $U_{12} = U_{13} = U_{23} = 0$ for all atoms.

TABLE 3
Select Interatomic Distances (Å) and Angles for $CeIrIn_5$, $CeRhIn_5$, and $CeIn_3$

$CeIrIn_5$ ($P4/mmm$)		$CeRhIn_5$ ($P4/mmm$)		$CeIn_3$ ($Pm\bar{3}m$)	
Unit cell constants (Å)		Unit cell constants (Å)		Unit cell constants (Å)	
a	4.674(1)	a	4.656(2)	a	4.689(2)
c	7.501(5)	c	7.542(1)		
[$CeIn_3$] cuboctahedra		[$CeIn_3$] cuboctahedra		$CeIn_3$ cuboctahedra	
Interatomic distances (Å)		Interatomic distances (Å)		Interatomic distances (Å)	
Ce–In1 × 4	3.3050(7)	Ce–In1 × 4	3.2923(14)	Ce–In × 12	3.3156(6)
Ce–In2 × 8	3.2717(11)	Ce–In2 × 8	3.2775(7)		
Angles (°)		Angles (°)		Angles (°)	
In1–Ce–In1	90(0)	In1–Ce–In1	90(0)	In–Ce–In	90(0)
In1–Ce–In2	59.662(11)	In1–Ce–In2	59.851(7)	In–Ce–In	60(0)
In1–Ce–In2	120.338(11)	In1–Ce–In2	120.149(7)	In–Ce–In	120(0)
In2–Ce–In2	91.17(4)	In2–Ce–In2	90.517(26)	In–Ce–In	90(0)
In2–Ce–In2	60.675(23)	In2–Ce–In2	60.298(15)	In–Ce–In	60(0)
In2–Ce–In2	88.83(4)	In2–Ce–In2	89.483(26)	In–Ce–In	90(0)
[$IrIn_2$] parallelepipeds		[$RhIn_2$] parallelepipeds			
Interatomic distances (Å)		Interatomic distances (Å)			
Ir–In2 × 8	2.7560(7)	Rh–In2 × 8	2.7500(9)		
Angles (°)		Angles (°)			
In2–Ir–In2	73.682(17)	In2–Rh–In2	73.539(11)		
In2–Ir–In2	64.02(4)	In2–Rh–In2	64.325(23)		

Note. The cell constant for $CeIn_3$ was taken from Ref. (33).

Data reduction and refinement of the structure. The X-ray diffraction data of $CeRhIn_5$ were corrected for Lorentz polarization and anisotropic absorption effects, by taking into consideration the dimensions and the Miller indices of the faces of the crystal. The intensity and reciprocal space position of the reference reflections showed no significant evolution during the data collection. Then, the 847 data were merged in the point group 4/*mmm*, resulting in 131 independent reflections. Full-matrix least-squares refinement of the crystal structure, based on F^2, was performed using the least-squares refinement program SHELXTL (31). Statistical weights were used and all 131 reflections were included in the refinement. Initially, only the scale factor was refined. Then, the refinement procedure is identical to the one described for $CeIrIn_5$. The applied extinction

TABLE 4
Parameters of the Least-Squares Refinement of the Single Crystal X-ray Diffraction Data

Number of reflections (all data)	847
Number of independent reflections	131
Number of parameters varied	12
θ range for data collection (°)	2.7–26.31
Extinction parameter g (rad^{-1})	$g = 0.14(2)$
Absorption coefficient (cm^{-1})	$\mu = 264.55$
$R1$	0.056
$wR2$	0.1152
GOF $\equiv \chi^2$ (based on F^2)	1.674

Note. $R1 = \sum||F_{obs}| - |F_{calc}||/\sum|F_{obs}|$, $wR2 = [\sum[w(F^2_{obs} - F^2_{calc})^2]/\sum[w(F^2_{obs})^2]]^{1/2}$, and GOF $\equiv \chi^2 = \sum[w(F^2_{obs} - F^2_{calc})^2]/(N_{obs} - N_{var})$, where N_{obs} = number of observations, N_{var} equals number of variables and $w = 1/\sigma^2(F^2_{obs}) + 0.1$.

correction covers both primary and secondary extinction (32). The parameters of the least-square refinement are given in Table 4 and the results from the crystal structure analysis are listed in Table 5. Select interatomic distances and angles of $CeRhIn_5$ are compared with the corresponding ones of $CeIrIn_5$ and $CeIn_3$ in Table 3.

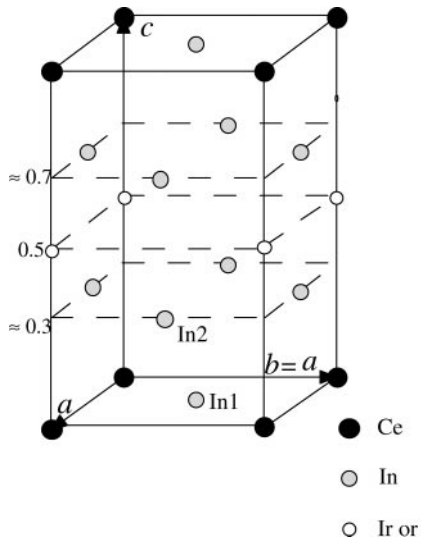

FIG. 2. Unit cell of $CeIrIn_5$ or $CeRhIn_5$. In2 and Rh atoms are on planes (indicated by dashed lines) at $z \approx 0.3$ and 0.5, respectively.

III. DISCUSSION

The unit cell of $CeIrIn_5$ and $CeRhIn_5$ is shown in Fig. 2. The basic structural units (coordination polyhedra) of the

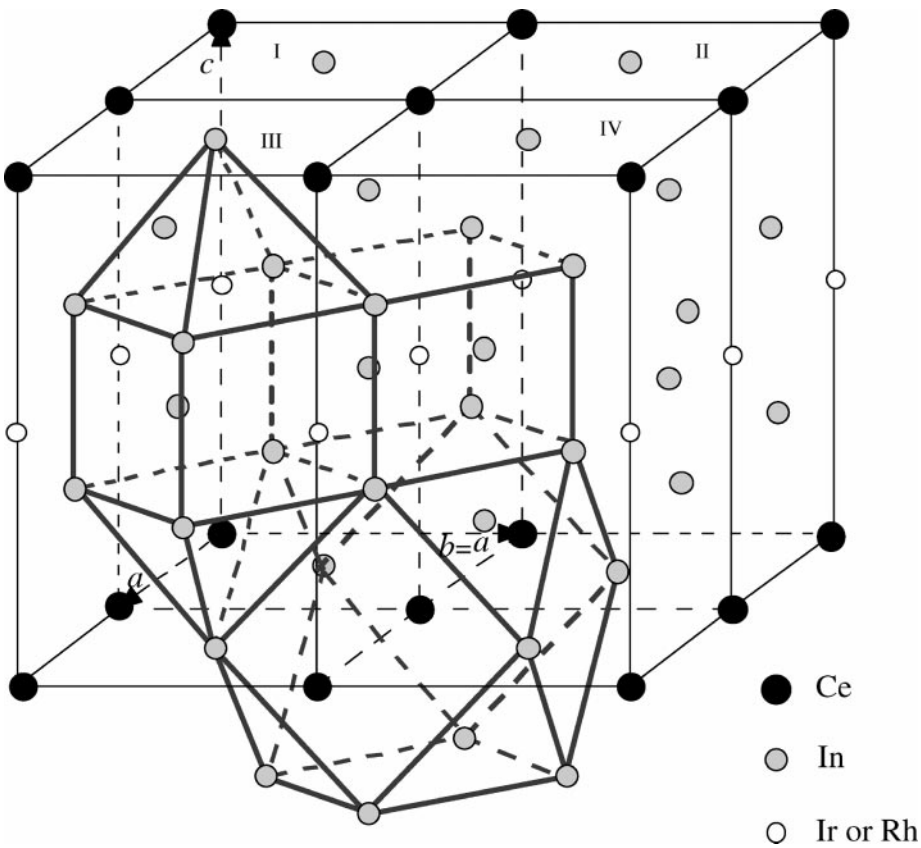

FIG. 3. The parent structures of $CeIrIn_5$ and $CeRhIn_5$: distorted [$CeIn_3$] cuboctahedra and [$IrIn_2$] or [$RhIn_2$] rectangular parallelepipeds. An empty elongated square dipyramid is also shown. All atoms of four unit cells are shown.

TABLE 5
Atomic Coordinates and Thermal Factors for $CeRhIn_5$

Atom	x	y	z	U_{11} (Å^2)	U_{22} (Å^2)	U_{33} (Å^2)
Ce	0	0	0	0.009(2)	0.009(2)	0.005(2)
Rh	0	0	0.5	0.002(1)	0.002(1)	0.010(2)
In1	0.5	0.5	0	0.014(2)	0.014(2)	0.011(2)
In2	0	0.5	0.3059(2)	0.018(2)	0.008(1)	0.007(2)

Note. $U_{12} = U_{13} = U_{23} = 0$ for all atoms.

structure are $[CeIn_3]$ cuboctahedra and $[IrIn_2]$ or $[RhIn_2]$ rectangular parallelepipeds (Fig. 3). A comparison of the main interatomic distances of $CeIrIn_5$, $CeRhIn_5$, and $CeIn_3$ (Table 3) reveals that, in $CeIrIn_5$ and $CeRhIn_5$, the $[CeIn_3]$ cuboctahedra are significantly distorted compared with the cubic $CeIn_3$. $[CeIn_3]$ cuboctahedra are more distorted in $CeIrIn_5$ than in $CeRhIn_5$. It is worth noting that this comparison among the interatomic distances of the three compounds is reliable despite the fact that they were deduced by different diffraction techniques. The reason is that it is well established by now (34) that for simple inorganic compounds there is very good agreement between positional parameters determined by single-crystal TOF neutron and single-crystal X-ray diffraction. In contrast, the correspondence between the temperature factors is much less satisfactory for data taken at room temperature because thermal diffuse scattering can seriously affect the thermal parameters. Thermal diffuse scattering corrections could not be applied to our data because not only the experimental conditions but also the elastic constants of the materials have to be known. Also, anharmonic atomic motions can affect the thermal parameters. Both effects are responsible to a large extent for the inadequate correspondence between the two sets of U_{ij}'s listed in Tables 2 and 5, despite the great care taken at every step of data collection, data reduction, and nuclear and electronic structure refinement. In addition, U_{ij}'s correspond to two different compounds and obviously deviations in their structural parameters are expected to some degree. It is quite remarkable, however, that for both materials, U_{11} of In2 is relatively large. U_{11} represents the thermal vibration of In2 along the c axis. Such a large atomic displacement factor could be due to either static or dynamic disorder. Static disorder would result in weak superlattice reflections that should be observed by electron diffraction. Since no such reflections have been detected by our electron diffraction experiments, the large U_{11} can be attributed to dynamical disorder of In2 along the c axis.

We now turn to the quasi-two-dimensional nature of the crystal structure $CeIrIn_5$ and $CeRhIn_5$ as illustrated in Fig. 4. This structure can be described as alternate stacking in the [001] direction of monolayers of distorted

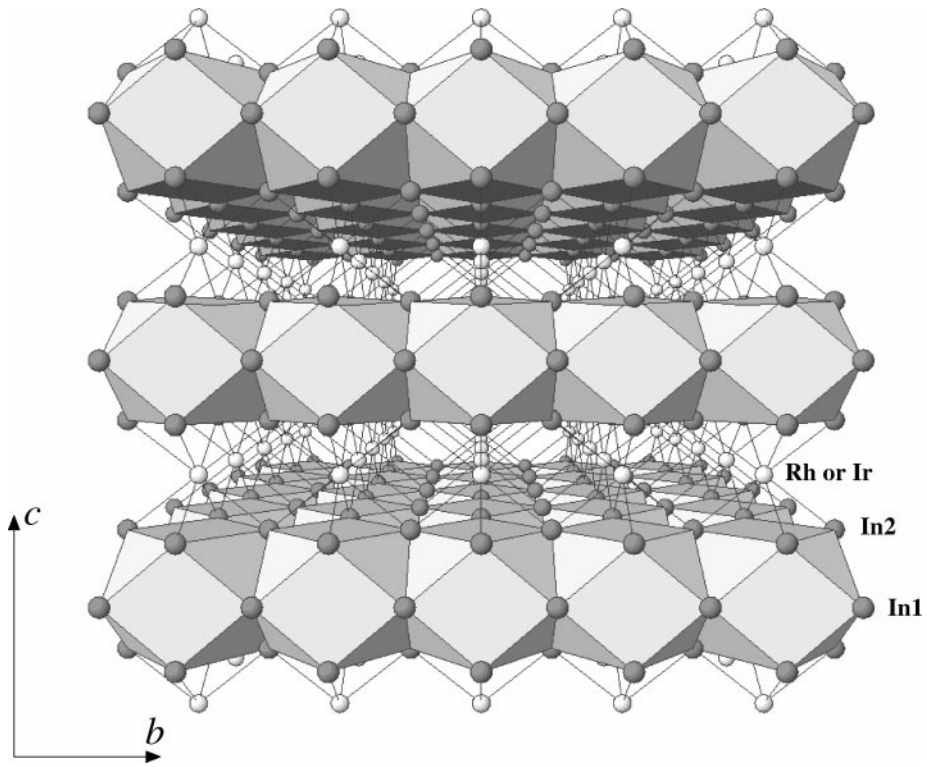

FIG. 4. The quasi 2D crystal structure of $CeIrIn_5$ and $CeRhIn_5$ viewed along [100]. Because of the tetragonal structure $a = b$. The Ce atoms are at the center of the distorted cuboctahedra $[CeIn_3]$.

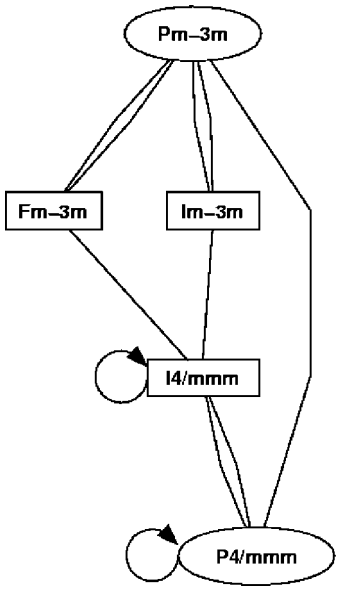

FIG. 5. Graphical representation of the group–subgroup relationship for the structures of $CeIn_3$ and $CeIrIn_5$ or $CeRhIn_5$. One edge means that there is a group-subgroup relation between the corresponding space groups. Two edges mean that there is a group–subgroup relation between these space groups in the two directions. The symbol that connects a space group by itself means that this space group has an isomorphic subgroup.

face-sharing cuboctahedra [$CeIn_3$] and monolayers of edge-sharing rectangular parallelepipeds [$IrIn_2$] or [$RhIn_2$]. The distortion of the [$CeIn_3$] cuboctahedra means that the [$CeIn_3$] layers are under chemical pressure induced by their adjacent [$IrIn_2$]- or [$RhIn_2$]-type layers. This arrangement of the occupied polyhedra leaves empty elongated square dipyramids, which have their long axis parallel to the c axis and are alternated with filled right parallelepipeds in their own [$IrIn_2$]- or [$RhIn_2$]-type slab.

The structure and composition of $CeRhIn_5$ and $CeIrIn_5$ implies, as already mentioned in the Introduction, that both materials are new members of the inhomogenous linear homologous series $M_mT_nT'_{3m+2n}$ initially reported by Grin *et al.* (8). The $M_mT_nT'_{3m+2n}$ compounds exist as well-defined phases whose structures consist of periodic intergrowths of segments of two simple parent structures: $AuCu_3$-type cuboctahedra [MT_3] and $PtHg_2$-type rectangular parallelepipeds [TT'_2]. The only members of the series that have been previously reported are for $m = n = 1$ (MTT'_5) (Refs. (8, 25, 35–40)) and for $m = 2$, $n = 1$ ($M_2TT'_8$) (Refs. 8, 36, 40–42)) (M: rare earth, Y, or U; T: group VIII metal; and T': Ga or In). All known $M_mT_nT'_{3m+2n}$ compounds adopt tetragonal structure (deduced mainly from conventional powder X-ray diffraction data) and are formed by n [TT'_2]-type and m [MT_3]-type layers alternatively stacked along the c axis. As a side remark, we mention that, among these materials, the system U–T–Ga (T: Co, Ni, Ir, Pd, Cu, Ru) has been investigated (37–40) as a strong candidate for heavy electron behavior but no such behavior has been found.

The interpretation of the structure of $CeIrIn_5$ and $CeRhIn_5$ by the intergrowth concept and the demonstration by our diffraction experiments that the materials are structurally ordered reveal that a sort of "crystal or lattice engineering" was achieved in the lattice of the cubic heavy fermion material $CeIn_3$: the dimensionality of three in $CeIn_3$ could be lowered to approximately two in $CeIrIn_5$ and $CeRhIn_5$ by separating compact monolayers of $CeIn_3$ from one another with insertion among them of the appropriate amount of Rh or Ir. To our knowledge, $CeIn_3$ is the first example in the class of heavy fermion materials where lowering of spatial dimensionality could be realized by the way just described.

The lowering of dimensionality is also depicted in the group–subgroup relationship for the structures of $CeIn_3$ and $CeIrIn_5$ or $CeRhIn_5$. The space group $P4/mmm$ of $CeIrIn_5$ and $CeRhIn_5$ is the maximal subgroup of the space group $Pm\bar{3}m$ of $CeIn_3$. The lattice of maximal subgroups for the group–subgroup pair ($Pm\bar{3}m$, $P4/mmm$) was deduced by using Refs. (43, 44) and is shown in Fig. 5. Intermediate subgroups that could relate $Pm\bar{3}m$ and $P4/mmm$ exist but no $M_mT_nT'_{3m+2n}$ compound is known to belong to any of these subgroups.

Finally, we comment briefly about the possible effects of the reduced dimensionality on the low-temperature physical properties of $CeRhIn_5$ and $CeIrIn_5$. Their 3D analogue, $CeIn_3$, is a heavy fermion antiferromagnet at ambient pressure, with Néel temperature, T_N, that evolves monotonically with application of external pressure and vanishes at about 25 kbar. At this pressure, superconductivity sets in at $T_c = 0.25$ K. This evolution of T_N as a function of pressure has been predicted theoretically by a currently widely accepted theoretical model (7) and it has also been observed in several other heavy fermion materials, which provided a general validation of the theoretical model. In striking contrast to $CeIn_3$ (and to all previously reported examples), $CeRhIn_5$ exhibits a first-order-like transition from an antiferromagnetic to superconducting state ($T_c = 2.5$ K) at critical pressure $14.9 \leq P_c \leq 16.3$ kbar (mentioned already at the Introduction). A qualitative explanation of this behavior stems from the structural characteristics of $CeRhIn_5$. By taking into consideration the bulk modulus $B = 650$ kbar for $CeIn_3$ (45), the difference in the cell parameters a of $CeRhIn_5$ and $CeIn_3$ implies that in $CeRhIn_5$ the building blocks [$CeIn_3$] are under chemical pressure of about 14 kbar relative to $CeIn_3$ at atmospheric pressure. Since the T_N of $CeIn_3$ becomes zero above approximately 25 kbar, an additional external pressure of at least about 11 kbar is required to drive T_N of $CeRhIn_5$ to zero. This value of the external pressure is close to the P_c of $CeRhIn_5$ defined above. The exact critical point P_c results from a competition between an increasing with pressure interlayer magnetic

exchange $J_\perp$ and a decreasing with pressure spin coupling (coupling among the 4*f* and conduction electrons). Further details on the low-temperature physical behavior of $CeRhIn_5$ are discussed in Ref. (6).

Our study of the way in which cooperative phenomena are influenced by the lowering of dimensionality in the heavy fermion superconductor $CeIrIn_5$ is still in progress. However, we mention here that perhaps the most interesting observation is an increase of the bulk T_c from ≈ 0.4 to ≈ 1 K when Ir is substituted by Rh. The $T_{c,max}$ corresponds to $CeIr_{\approx 0.25}Rh_{\approx 0.75}In_5$. Similar behavior has been observed in the other class of quasi-2D strongly correlated electron materials, namely, the high-T_c superconductors. A detailed discussion of the appealing and intriguing properties of $CeIrIn_5$ is given in Ref. (5).

We are extending our investigation to other members of this fascinating and unexplored intergrowth homologous series to more deeply investigate the evolution of the structure and the properties among the various members of the series.

ACKNOWLEDGMENTS

E.G.M. thanks A. J. Schultz for assistance during the neutron data collection and fruitful discussions and Brian Scott for making available the X-ray single-crystal diffractometer. She also thanks Cedomir Petrovic for useful discussions. Work at Los Alamos National Laboratory was performed under the auspices of the U.S. Department of Energy. Work at Brookhaven National Laboratory was supported by the U.S. Department of Energy, Division of Materials Sciences under Contract DE-AC02-98CH10886. This work has benefited from the use of the Intense Pulsed Neutron Source, Argonne National Laboratory. This facility is funded by the U.S. Department of Energy, BES-Materials Science, under Contract W-31-109-Eng-38.

REFERENCES

1. Z. Fisk, H. R. Ott, and J. L. Smith, *J. Less Common Met.* **133,** 99 (1987).
2. Z. Fisk, J. D. Thompson, and H. R. Ott, *J. Magn. Magn. Mater.* **76&77,** 637 (1988).
3. H. R. Ott and Z. Fisk, *ACS Symp. Ser.* **394,** 260 (1989).
4. R. B. King, *J. Solid State Chem.* **131,** 394 (1997).
5. C. Petrovic, R. Movshovich, M. Jaime, P. G. Pagliuso, M. F. Hundley, J. L. Sarrao, Z. Fisk, and J. D. Thompson, submitted.
6. H. Hegger, C. Petrovic, E. G. Moshopoulou, M. F. Hundley, J. L. Sarrao, Z. Fisk, and J. D. Thompson, *Phys. Rev. Lett.* **84,** 4986 (2000).
7. S. Doniach, *in* "Valence Instabilities and Related Narrow Band Phenomena" (R. D. Parks, Ed.), p. 169. Plenum, New York, 1977. S. Doniach, *Physica B* **91,** 231 (1977).
8. Y. N. Grin, Y. P. Yarmolyuk, and E. I. Giadyshevskii, *Sov. Phys. Crystallogr.* **24**(2), 137 (1979).
9. Z. Fisk and J. P. Remeika, *in* "Handbook on the Physics and Chemistry of Rare Earths," (K. A. Gschneider, Jr. and L. Eyring, Eds.), Vol. 12, p. 53. Elsevier, North-Holland, 1989.
10. K. Yvon, W. Jeitschko, and E. Parthé, *J. Appl. Crystallogr.* **10,** 73 (1977).
11. M. M. Hall, Jr., V. G. Veeraraghavan, H. Rubin, and P. G. Winchell, *J. Appl. Crystallogr.* **10,** 66 (1977).
12. G. K. Williamson and W. H. Hall, *Acta Metal.* **1,** 22 (1953). S. A. Howard and K. D. Preston, *in* "Modern Powder Diffraction" (D. L. Bish and J. E. Post, Eds.), pp. 266–268. Book Crafters, Chelsea, MI, 1989.
13. E. Bauer, H. Nowotny, and A. Stempfl, *Monatsh. Chem.* **84,** 693 (1953).
14. "Atlas of Crystal Structure Types for Intermetallic Phases" (J. L. C. Daams, P. Villars, and J. H. N. van Vucht, Eds.), Vol. 2, pp. 3541–3543. ASM International, Materials Park, OH, 1991.
15. B. G. Hyde and Sten Andersson, *in* "Inorganic Crystal Structures" pp. 189–190. Wiley, New York, 1989.
16. Z. Fisk, D. W. Hess, C. J. Pethick, D. Pines, J. L. Smith, J. D. Thompson, and J. O. Willis, *Science* **239,** 33 (1988).
17. M. F. Hundley, unpublished.
18. I. Takahashi, A. Kagayama, G. Oomi, Y. Onuki, and T. Komatsubara, *Acta Crystallogr. Sect. B* **55,** 31 (1999).
19. A. J. Schultz, *Trans. Am. Crystallogr. Assoc.* **23,** 61 (1987); **29,** 29 (1993).
20. A. J. Shultz and P. C. W. Leung, *J. Phys. (Paris)* **47**(C5), 137 (1986).
21. A. J. Shultz, K. Srinivasan, R. G. Teller, J. M. Williams, and C. M. Lukehart, *J. Am. Chem. Soc.* **106,** 999 (1984).
22. A. J. Shultz, "Single Crystal Diffractometer User's Guide and Reference Manual." ANL, Nov 1993.
23. R. A. Jacobson, *J. Appl. Crystallogr.* **19,** 283 (1986).
24. V. F. Sears, *Neutron News* **3,** 26 (1992).
25. Y. N. Grin, P. Rogl, and K. Hiebl, *J. Less-Common Met.* **121,** 497, (1986).
26. A. C. Larson and R. B. Von Dreele, "General Structure Analysis System," LAUR 86–748, Los Alamos National Laboratory, Los Alamos, NM, 1994.
27. P. J. Becker and P. Coppens, *Acta Crystallogr. Sect. A* **30,** 129 (1974).
28. B. T. M. Willis and A. W. Pryor, "Thermal Vibrations in Crystallography" pp. 102–110. Cambridge Univ. Press, Cambridge, U.K., 1975.
29. SMART, Version 4.210. Bruker Analytical X-Ray Systems, Madison, WI, 1996.
30. SAINT, Version 4.05. Bruker Analytical X-Ray Systems, Madison, WI, 1996.
31. SHELXTL, PC version 4.2/360. Bruker Analytical X-ray Instruments, Madison, WI, 53719.
32. A. C. Larson, *in* "Crystallographic Computing" (F. R. Ahmed, Ed.), pp. 291–294. Munksgaard, Copenhagen, 1970.
33. Jon Lawrence, *Phys. Rev. B* **20,** 3770 (1979).
34. P. Coppens, J. Dam, S. Harkema, D. Feil, R. Feld, M. S. Lehmann, R. Goddard, C. Krüger, E. Hellner, H. Johansen, F. K. Larsen, T. F. Koetzle, T. F. McMullan, E. N. Maslen, and E. D. Stevens, *Acta Crystallogr. Sect. A* **40,** 184 (1984). B. B. Iversen, F. K. Larsen, B. N. Figgis, P. A. Reynolds, and A. J. Schultz, *Acta Crystallogr. Sect. B* **52,** 923 (1996), and references therein.
35. Y. N. Grin, P. Rogl, and K. Hiebl, *in* "Actinides '85, Abstracts" p. 114. Aix de Province, 1985.
36. Y. M. Kalychak, V. I. Zaremba, V. M. Baranyak, V. A. Bruskov, and P. Y. Zavalii, *Russ. Metal.* **1,** 213 (1989).
37. V. Sechovsky, L. Havela, G. Schaudy, G. Hilscher, N. Pillmayr, P. Rogl, and P. Fischer, *J. Magn. Magn. Mater.* **104–107,** 11 (1992).
38. S. Noguchi and K. Okuda, *J. Magn. Magn. Mater.* **104–107,** 57 (1992).
39. S. Noguchi and K. Okuda, *Physica B* **188,** 749 (1993).
40. M. Schonert, S. Corsepius, E. W. Scheidt, and G. R. Stewart, *J. Alloys Compd.* **224,** 108 (1995).
41. Y. N. Grin, P. Rogl, L. G. Akselrud, V. K. Pecharskii, and Y. P. Yarmolyuk, *Russ. Metal.* **4,** 206 (1988).
42. R. V. Lapunova, Y. N. Gryn, and Y. P. Yarmolyuk, *Dop. Ak. Nauk Ukr. RSR Ser. B Transl.* **8,** 43 (1984).
43. "International Tables for Crystallography" (T. Hahn, Ed.), Kluwer, Dordrecht, 1996.
44. Program SUBGROUPGRAPH, Bilbao Crystallographic Server, http://www.cryst.ehu.es/.
45. G. Oomi, T. Kagayama, and J. Sakurai, *J. Mater. Process. Technol.* **85,** 220 (1999).